# Combining ALMA with HST and VLT to Find the Counterparts of Submillimetre Galaxies

Tommy Wiklind[1]
Christopher J. Conselice[2]
Tomas Dahlen[3]
Mark E. Dickinson[4]
Henry C. Ferguson[3]
Norman A. Grogin[3]
Yicheng Guo[5]
Anton M. Koekemoer[3]
Bahram Mobasher[6]
Alice Mortlock[2]
Adriano Fontana[7]
Romeel Davé[8,9,10]
Haojing Yan[11]
Viviana Acquaviva[12]
Matthew L. N. Ashby[13]
Guillermo Barro[5]
Karina I. Caputi[14]
Marco Castellano[7]
Avishai Dekel[15]
Jennifer L. Donley[16]
Giovanni G. Fazio[13]
Mauro Giavalisco[17]
Andrea Grazian[7]
Nimish P. Hathi[18]
Peter Kurczynski[19]
Yu Lu[20]
Elizabeth J. McGrath[21]
Duilia F. de Mello[22]
Michael Peth[23]
Mohammad Safarzadeh[23]
Mauro Stefanon[11]
Thomas Targett[24,25]

[1] ESO/Joint ALMA Observatory, Santiago, Chile
[2] Department of Physics and Astronomy, University of Nottingham, United Kingdom
[3] Space Telescope Science Institute, Baltimore, USA
[4] National Optical Observatory, Tucson, USA
[5] UCO/Lick Observatory, Department of Astronomy and Astrophysics, University of California, Santa Cruz, USA
[6] Department of Physics and Astronomy, University of California, Riverside, USA
[7] INAF–Osservatorio Astronomico di Roma, Monteporzio, Italy
[8] University of the Western Cape, Bellville, South Africa
[9] South African Astronomical Observatories, Cape Town, South Africa
[10] African Institute for Mathematical Sciences, Muizenberg, South Africa
[11] Department of Physics and Astronomy, University of Missouri, Columbia, USA
[12] Physics Department, CUNY New York City College of Technology, Brooklyn, USA
[13] Harvard-Smithsonian Center for Astrophysics, Cambridge, USA
[14] Kapteyn Astronomical Institute, University of Groningen, the Netherlands
[15] Center for Astrophysics and Planetary Science, Racah Institute of Physics, The Hebrew University, Jerusalem, Israel
[16] Los Alamos National Laboratory, USA
[17] Department of Physics and Astronomy, University of Massachusetts, Amherst, USA
[18] Aix Marseille Université, CNRS, Laboratoire d'Astrophysique de Marseille, France
[19] Department of Physics and Astronomy, Rutgers, The State University of New Jersey, Piscataway, USA
[20] Kavli Institute for Particle Astrophysics & Cosmology, Stanford, USA
[21] Department of Physics and Astronomy, Colby College, Waterville, USA
[22] Department of Physics and Astronomy, Catholic University of America, Washington, USA
[23] Department of Physics and Astronomy, Johns Hopkins University, Baltimore, USA
[24] Institute for Astronomy, University of Edinburgh, Royal Observatory, Edinburgh, United Kingdom
[25] Department of Physics and Astronomy, Sonoma State University, Rohnert Park, USA

**The identification of optical/near-infrared counterparts to submillimetre galaxies (SMGs) has been one of the most enduring obstacles in learning more about the nature of these massively star-forming systems, including their true redshift distribution. Various techniques have been partially successful but it is only by imaging the submillimetre (submm) emission at the same angular resolution as the optical images that counterparts can be securely assigned. With ALMA it is now possible to image the redshifted dust emission from these objects with a minimum investment of observing time. The results of an analysis of the properties of the counterparts of ten submm galaxies that fall within the CANDELS coverage of the GOODS-S field is presented. All ten SMGs show homogeneous properties in their dust and gas content, but only eight show (surprisingly) homogeneous properties in terms of the stellar mass and characteristic age of the stellar population. The two deviating counterparts are discussed.**

From the very beginning, the formidable angular resolution of the Hubble Space Telescope (HST) was a benchmark used in the planning for the Atacama Large Millimeter/Submillimeter Array (ALMA). With the same angular resolution at submillimetre (submm) wavelengths as in the optical, it is possible to study the cold Universe on the same scales as with HST and to make a detailed multi-wavelength comparison of the cold and hot components of astrophysical objects. This quest for high angular resolution was a driver pushing the ALMA array to both shorter wavelengths and to accommodate longer baselines. In the end, the angular resolution of ALMA will surpass that of HST, although it will take some more testing and verification of ALMA's performance before this becomes a standard observing mode.

The ability to combine the input from different telescopes to allow multi-wavelength coverage with comparable angular resolution, stretching from optical/ultraviolet (UV) through millimetre wavelengths, enables us to better understand the physical processes governing a range of astrophysical phenomena. There are, however, cases where the mere identification of optical counterparts to radio-detected sources, viewed at similar angular resolution, is a big achievement. One such class of objects is the elusive submm galaxies initially detected through their continuum emission at submm wavelengths. This emission originates as redshifted thermal emission from dust grains heated by UV photons, and probes the presence of young and massive stars and/or the presence of a dust-embedded active galactic nucleus (AGN).

## Submm galaxies and the quest for optical counterparts

The possibility of detecting redshifted far-infrared (FIR) emission at submm wave-

lengths was discussed in a seminal paper by Andrew Blain and Malcolm Longair (Blain & Longair, 1993). The first bolometer array with a wavelength coverage and sensitivity to detect this high-redshift FIR emission was SCUBA (Submm Common User Bolometer Array), which was used on the 15-metre single-dish James Clerk Maxwell Telescope (JCMT) from 1997 until 2005. Some of the first projects pursued with SCUBA were to search for redshifted FIR emission towards the Hubble Deep Field (HDF) North and toward lensing clusters (Hughes et al., 1998; Smail et al., 1997). Several submm sources were detected, but identifying the optical counterparts proved to be very difficult due to the poor angular resolution achieved with the JCMT/SCUBA combination, resulting in a positional accuracy of ~ 15 arcseconds.

During the following decade several methods were employed to pinpoint the optical counterparts of SMGs and/or to estimate their redshift distribution. By pushing radio continuum observations to a sensitivity level where massive star formation is the main contributor to the continuum emission, and using radio interferometers to achieve sub-arcsecond angular resolution, it was possible to identify the counterparts of some SMGs and thereby obtain optical spectroscopic observations (Chapman et al., 2003; Arextaga et al., 2007). This method, however, can only account for a subset of all SMGs. A significant fraction of SMGs remained undetected even in the deepest radio continuum observations, possibly due to being at high redshift where the radio continuum falls below the detection limit, and some galaxies do not reveal optical emission so no spectroscopy can be done. An illustrative example of an elusive SMG is the brightest submm source in the HDF North (Hughes et al., 1998). Despite a large observational effort, no optical or near-infrared (NIR) counterpart has yet been identified. The redshift was only recently determined using rotational CO emission lines, and found to be $z$ ~ 5.2 (Walter et al., 2012).

Several other methods have been used to find the counterparts of SMGs, most notably association via near-infrared and far-infrared emission (e.g., Targett et al. [2013] and references therein). However, these methods, while partially successful, have the common thread that they are indirect methods and thus prone to potential biases and misidentifications. Despite this, our knowledge of the properties of the submm galaxy counterparts has grown, albeit slowly and at a huge cost in telescope time.

It is really only through the use of submm interferometry, targeting the same emission as seen with bolometers, that the positional accuracy of the FIR emission can be determined with enough accuracy to allow a direct association of the optical counterpart, thus eliminating the potential for misidentifications and biases. This approach was pioneered with the SMA (SubMillimeter Array), IRAM's (Institut de Radioastronomie Millimetrique) Plateau de Bure and CARMA (Combined Array for Research in Millimeterwave Astronomy) telescopes. This approach, however, has been a time-consuming exercise, requiring up to eight hours of observing time per source. Hence, only a limited number of counterparts have been identified using this method. This is where ALMA, with its unprecedented sensitivity and high angular resolution, is a true game changer.

## First results on SMGs with ALMA

During the very first cycle of ALMA Early Science (Cycle 0), one project (2011.0.00294.S) used the 16 available antennas to observe dust continuum emission at 870 µm towards 126 submm galaxies in the Extended Chandra Deep Field South (ECDFS). These submm galaxies were first identified using the Large Array Bolometer CAmera (LABOCA) bolometer on the Atacama Pathfinder EXplorer (APEX) telescope (Weiss et al., 2009). The ALMA observations and the results have been described by Swinbank et al. (2012) and in Hodge et al. (2013).

In short, with only ~ 2 minutes of observing time per source, both the sensitivity and the angular resolution were substantially improved compared to previous observations. The ALMA data was obtained in a compact configuration, resulting in a typical angular resolution of 1.6 by 1.1 arcseconds. The positional accuracy of the centre of the emission is, in most cases, 0.2–0.3 arcseconds (Hodge et al., 2013). Several instances of multiple submm sources within a single LABOCA "footprint" were found, and quite often, the submm emission was found to be offset from the centre of the LABOCA position (see Figure 1 in Swinbank et al., 2012).

A note on naming and the designation of the SMGs: the submm sources detected in the ECDFS with APEX/LABOCA are designated LESS (LABOCA ECDF Submillimeter Survey) followed by a number. The sources observed with ALMA are designated as ALMA-LESS # or ALESS #. The correct International Astronomical Union designation for these sources is, for instance, LESS J033219.0-275219. Here we will refer to the sources as LESS #, and use ALESS # when specifically addressing the submm emission observed with ALMA.

## Combining ALMA with HST and VLT

In Wiklind et al. (2014) we used the results presented in Hodge et al. (2013) to identify optical/NIR counterparts to the ALESS sources within the Great Observatories Origins Deep Survey South (GOODS-S) field. The counterparts were analysed in terms of their physical properties, morphology and environment using the data amassed within the Cosmic Assembly Near-infrared Deep Extragalactic Legacy Survey (CANDELS) project.

The GOODS-S field is located within the ECDFS and is one of five fields observed in the CANDELS project. The CANDELS data (Grogin et al., 2011; Koekemoer et al., 2011) provides very deep near-infrared imaging using the Wide-Field Camera 3 (WFC3) installed on HST in 2009. Deep *K*-band data was provided through the VLT Hawk-I instrument and the HAWK-I Ultra Deep Survey and GOODS Survey (HUGS; Fontana et al., 2014). Overall, the CANDELS survey provides photometric data in 18 bands ranging from UV to mid-infrared. The data contains UV (VLT/VIMOS), optical (HST/ACS), and infrared (HST/WFC3, VLT/ISAAC, VLT/HAWK-I and Spitzer/IRAC) photometry (Ashby et al., 2013). A catalogue (Guo et al., 2013) was made based on source detection in the WFC3 F160W band. Photometry in bands other than WFC3 F160W is measured

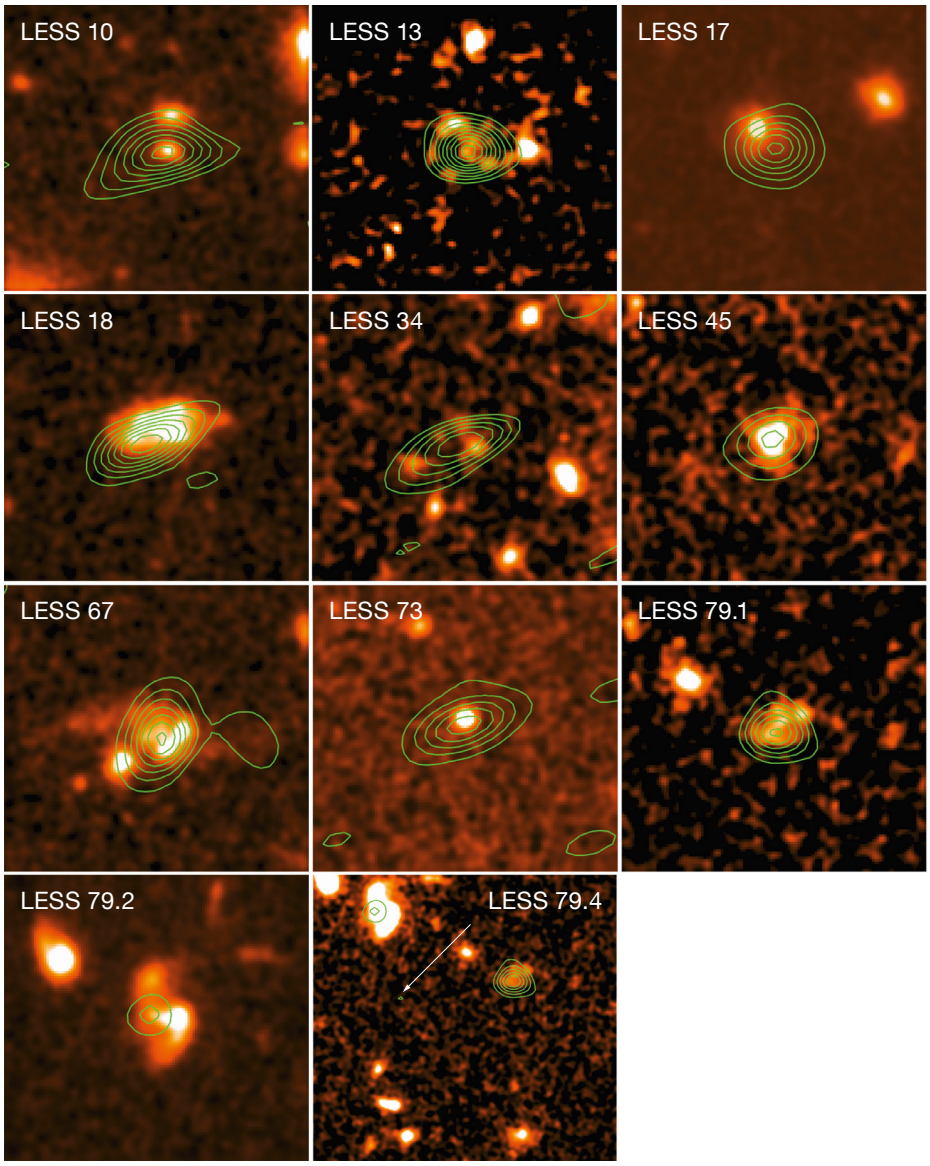


Figure 1. HST/WFC3 F160W images of the ten SMGs with identified counterparts in the CANDELS coverage of the GOODS-S field. Each image is ~ 7 by 7 arcseconds and has been smoothed to enhance the faint NIR emission. Contours show the ALMA 870 μm continuum emission, with contours starting at 0.1 mJy/beam and in steps of 0.1 mJy. The last image shows ALESS 79.4 (Hodge et al., 2013), which is much fainter than any of the other submm sources and has no identified counterpart.

using point spread function matching. Photometry of lower resolution images is done using the TFIT template-fitting method (see Guo et al. [2013] and references therein). The CANDELS survey also includes Spitzer/MIPS 24 μm data (Magnelli et al., 2011).

The *H*-band selected catalogue contains 34 930 sources with the representative 50 % completeness reaching 25.9, 26.6 and 28.1 AB mags in the F160W band for three different regions. The sources were extracted using SExtractor. Thirteen of the 126 LESS sources are located within the GOODS-South field as defined by the CANDELS coverage. ALMA observed nine of these. Hodge et al. (2013) reported multiple submm emission regions for three of the nine LESS sources within the WFC3/F160W area, for a total of 14 submm emission sources. Due to low signal-to-noise we retained only one of these multiple regions as a true individual SMG. Therefore the total number of individual SMG sources analysed was ten.

## Identifying the counterparts

We identified the optical/NIR counterparts to the ALESS sources by matching the coordinates of the submm sources seen with ALMA (Hodge et al., 2013) with galaxies in the CANDELS WFC3 F160W selected catalogue (Guo et al., 2013). Given ALMA's positional accuracy of 0.2–0.3 arcseconds, combined with the 0.06-arcsecond pixel scale of the HST data, ensures that we can securely connect the SMGs with their nearest optical/NIR counterparts. There are, however, two caveats. The central location of the submm emission may not coincide with the centre of optical/near-infrared emission due to strong dust extinction. This effect has been seen in other submm galaxies and is exacerbated with increasing redshift, as shorter wavelength emission is shifted into a given optical/NIR filter. We must therefore allow for coordinate offsets of the order of 0.5 arcseconds, or ~ 4.5 kpc at $z$ ~ 2. The second caveat is the possible, although improbable, coincidence of a background SMG with a foreground galaxy. While this is unlikely for the small sample discussed here, the fact that the initial LABOCA survey is luminosity limited creates a bias towards sources that may be gravitationally magnified by a foreground object.

The WFC3 counterparts to the ALESS sources are shown in Figure 1 together with contours of the submm emission observed with ALMA. From the figure it is clear that in most cases the position of the submm and NIR emission agrees quite well. There are, however, cases where the submm emission is offset from the NIR counterpart by up to 0.6 arcseconds, sometimes because the counterpart is part of a gravitationally interacting system (LESS 13, 67 and 79.2). Nevertheless, all of the submm sources were found to have a counterpart within 0.6 arcseconds of the centre of the submm emission with the exception of LESS 79.4 (Hodge et al., 2103). This submm source is faint and may be a spurious detection; it was not analysed in Wiklind et al. (2104).

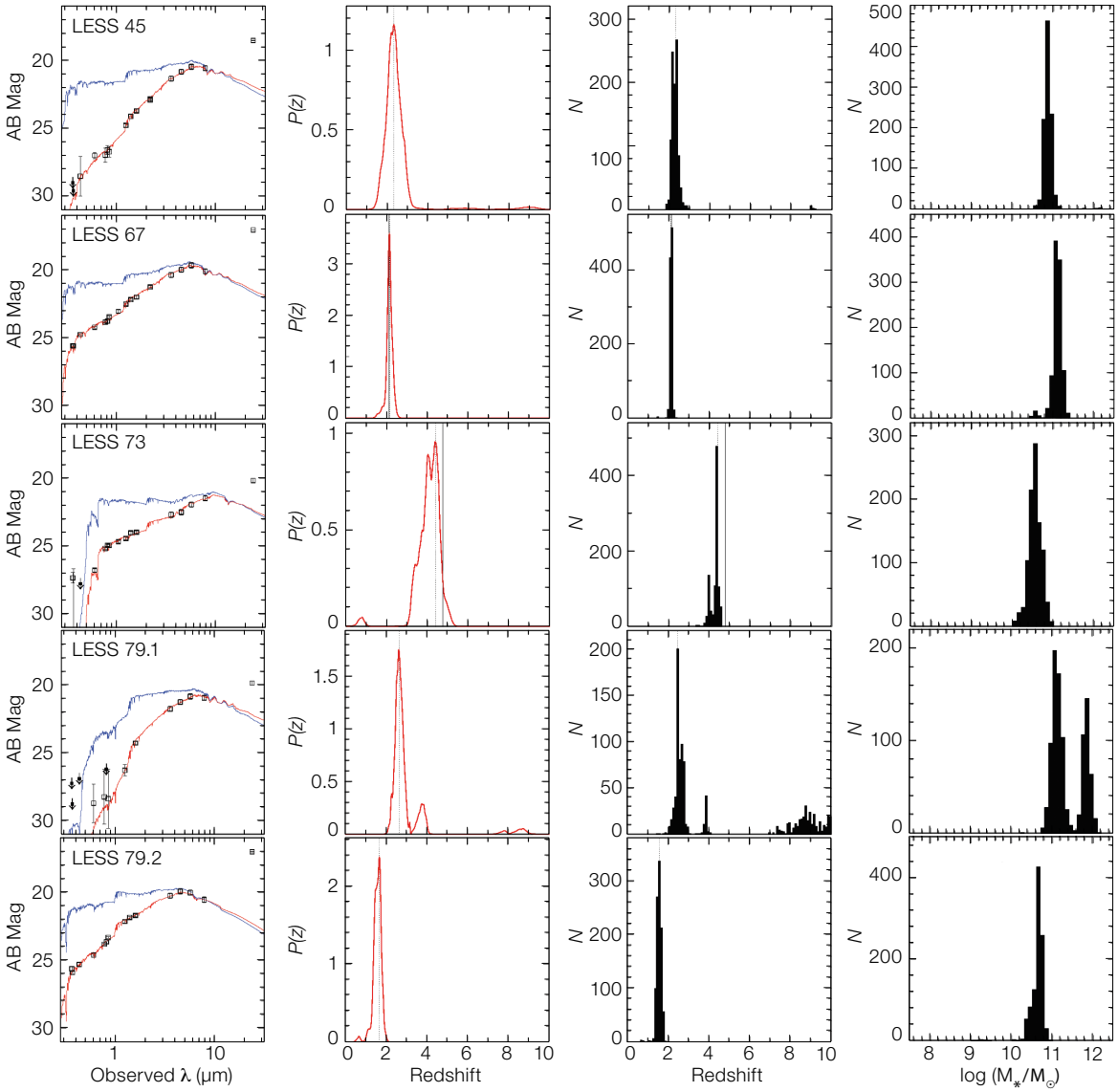


Figure 2. Results from the SED fitting of the UV through NIR photometry of the counterparts of the submm galaxies. The first column shows the actual SED, with the red line corresponding to the fit including dust obscuration and the blue line the corresponding SED corrected for dust extinction. The second and third columns show the probability distribution, *P(z)*, of the photometric redshift and the result from Monte Carlo simulations, respectively. The fourth column shows the simulation results for the stellar mass of the counterparts.

## Physical properties of the counterparts

With the counterparts identified, parameters, such as photometric redshift, stellar mass, characteristic age of the stellar population, extinction and metallicity were derived by fitting spectral energy distributions (SEDs) using the stellar population synthesis models of Bruzual & Charlot (2003) and the CANDELS data. For each counterpart we explored a large parameter space for redshift, stellar age, dust extinction and star formation history. The star formation history was parameterised as a delayed-$\tau$ model, which allows for an initial increase in the star formation rate, up to an age $t = \tau$, followed by a declining star formation rate. This form of the star formation history is superior to the simple exponentially declining star formation rate (cf., Lee et al., 2010). The SED-fitting algorithm and the star formation rate parameterisation are described in Wiklind et al (2014).

The stability of the SED fits with respect to photometric uncertainties was explored using Monte Carlo simulations, where the photometric values were allowed to vary stochastically within their nominal errors. For each galaxy the result gives an estimate of the confidence of the various solutions with respect to the photometric values and uncertainties. For each solution of a photometric redshift, we also constructed a probability distribution *P(z)* representing the uncertainty of the photometric redshift associated with the fitting of a single set of photometric values. Combining the *P(z)* distributions from the Monte Carlo simulations gives a probability distribution that also takes the stability of the solutions into consideration. Examples of the results from the Monte Carlo simulations as well as the probability distributions for the photometric redshifts and stellar masses are shown in Figure 2.

The Bruzual & Charlot (2003) models only include stellar components and are not

designed to model an AGN contribution to the SED. Since a substantial fraction of SMGs are known to contain an AGN (e.g., Donley et al., 2010), the SED-fitting results could be biased by the UV contribution of the AGN. This would be handled by the SED fit as a young stellar component and/or as having less extinction than actually is the case. However, this bias does not appear to be present in the SED-fitting results for the LESS sources, even though almost 50 % of them are designated as containing an AGN based on X-ray, radio and infrared signatures. In fact, the stellar populations of the SMGs are characterised by relatively evolved stars, with characteristic ages ranging from a few hundred Myr to 1–2 Gyr, as well as containing a significant amount of dust extinction. The photometric redshifts range from $z$ = 1.6 to $z$ = 4.7. At least two of the SMGs are located at $z$ > 4, while the average redshift for the remaining eight SMGs is ~ 2.0.

The stellar mass is estimated from the SED fit. This method has been shown to give robust mass estimates when compared with galaxies from semi-analytical models, where the mass of the stellar component is known (Lee et al., 2010). The stellar masses of the SMG counterparts are remarkably uniform, with two glaring exceptions. For eight of the SMGs the average stellar mass is $1 \times 10^{11}\ M_{\odot}$ with a surprisingly small dispersion, see Figure 3. The two remaining sources (LESS 10 and LESS 34) stand out with stellar masses almost two orders of magnitude smaller.

The most likely explanation of the two discrepant sources is that the submm emission originates from a background source not visible in the optical/NIR. Inspection of Figure 1 shows that this could very well be the case for LESS 34, where the submm emission is offset from the designated counterpart. For LESS 10, however, the submm emission and the counterpart are very well aligned and it is more difficult to consider this as a misaligned fore- or background source. Nevertheless, it is even less plausible that these two SMGs are in a different stage of evolution. In the case of LESS 34, the estimated stellar mass is actually smaller than the dust mass derived from the optically thin submm emission. This is clearly a contradiction and can be resolved if the submm emission originates in a background source, invisible in the optical/NIR images.

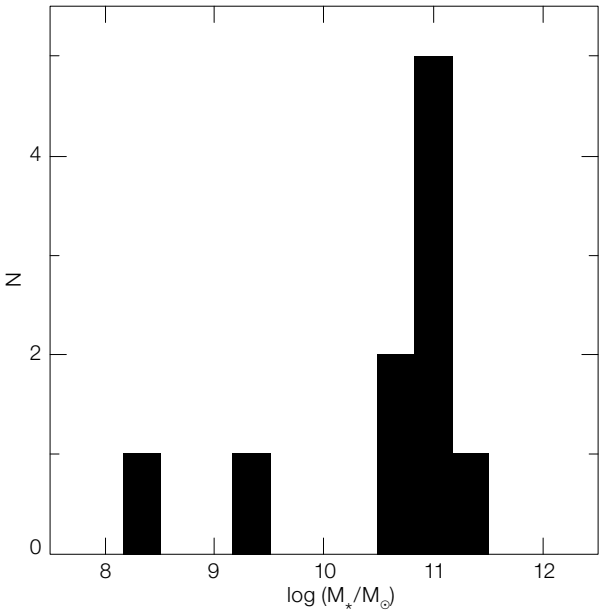


Figure 3. The distribution of stellar masses for the ten submm galaxies in the CANDELS GOODS-S coverage. The two low-mass galaxies are LESS 10 and LESS 34. In the case of LESS 34 ($\log(M_{*}/M_{\odot})$ ~ 8.4), the stellar mass is less than the estimated dust mass, which is clearly unphysical.

## Morphology of the counterparts

We measured the morphology of the SMG counterparts through both visual inspection of the HST images and by using non-parametric parameters (so called CAS — concentration, asymmetry and clumpiness). For this analysis we used the HST/WFC3 F160W images, in most cases corresponding to a restframe wavelength of ~ 5000 Å. The CAS parameters represent a non-parametric method for measuring the forms and structures of galaxies in resolved CCD images (for further details see Conselice et al., 2003). We also derive the Gini and $M_{20}$ coefficients for the SMGs. The Gini parameter is a statistical tool originally used to determine the distribution of wealth within a population, with higher values indicating a very unequal distribution. The $M_{20}$ parameter is similar to the concentration parameter (C) in that it gives a value that indicates if light is concentrated within an image; it is, however, calculated slightly differently from the C and Gini coefficients (e.g., Lotz et al., 2008).

From visual inspection, we designated an SMG counterpart as a merger if it shows signs of gravitational interaction and has tidal tails. If the counterpart has one or more neighbours within 30 kpc and $\Delta z \pm 0.1$, but without signs of interaction, we designate it as a neighbour. In the absence of any interaction and neighbour within 30 kpc, the SMG is designated as isolated. Of the ten SMG counterparts, only three show clear signs of being part of a merger system. This is in contrast to local ultraluminous infrared galaxies (ULIRGs), which are almost always part of merging systems.

In order to assess whether the asymmetry values of the SMGs are different from non-SMG galaxies of similar mass and at the same redshift, we constructed a control sample for each SMG, consisting of galaxies with stellar mass within ± 0.2 dex of that of the SMG and $\Delta z \pm 0.2$ of the photometric redshift of the SMG in question. The control galaxies were drawn from the same CANDELS GOODS-S F160W selected catalogue as the SMG counterparts. Comparing the asymmetry parameter values for the galaxies in the control samples with the SMGs shows that the three SMGs with the highest asymmetry parameter (LESS 34, 67 and 79.2) have values that are higher than 98 % of their respective control sample. The LESS 67 and LESS 79.2 counterparts show clear signs of merging, while LESS 34 is one of the sources with abnormally low stellar mass,

possibly because the counterpart is a foreground system.

We also did a Monte Carlo simulation where we compared the average asymmetry parameter of our SMGs with that of a randomised sample of galaxies and randomly selected ten galaxies, each appropriate to the control samples. The average asymmetry value of these ten galaxies was derived and compared with the average value of the SMGs. Repeating this procedure 1000 times, we find that in 99 % of the Monte Carlo realisations, the average asymmetry of the SMG counterparts is higher than the average asymmetry value of the control sample.

These results suggest that the SMGs are intrinsically more asymmetric than the typical galaxies at the same redshift and mass range. The small fraction of mergers among the SMG counterparts suggests that the high asymmetry is due to intrinsic clumpiness and/or patchy dust distribution (an example of a patchy dust distribution is shown in Figure 4) rather than being caused by gravitational interaction.

## Gas and dust properties

For redshifts low enough that the observed submm emission samples the Rayleigh–Jeans part of the dust SED, the emission is optically thin. For typical dust SEDs, this is the case as long as $z < 4$. In the optically thin case, the luminosity of the submm emission is a measure of the total dust mass. Adopting dust properties from a sample of local galaxies, we used the ALMA submm fluxes and our photometric redshift estimates to derive dust masses for the ALESS sources. The average dust mass is $(4.0 \pm 1.3) \times 10^8\ M_{\odot}$. As mentioned above, the dust mass of LESS 34 exceeds the estimated stellar mass, which is an argument for the SMG being a background source. It is also possible to empirically derive a conversion factor between the 870 μm luminosity and the gas mass (Scoville et al., 2014). This leads to very similar values of the dust mass as derived by simply assuming that the dust properties of the high-$z$ SMGs are similar to local galaxies.

Overall, the gas and dust properties of the SMGs are remarkably homogeneous, with a small dispersion. This is similar to the results obtained for the stellar masses, with the exception for the two deviating sources LESS 10 and LESS 34. The fact that these two sources appear to have normal SMG properties but deviate in the properties of their assigned counterparts further strengthens the suspicion that their true counterparts are background sources that remain undetected.

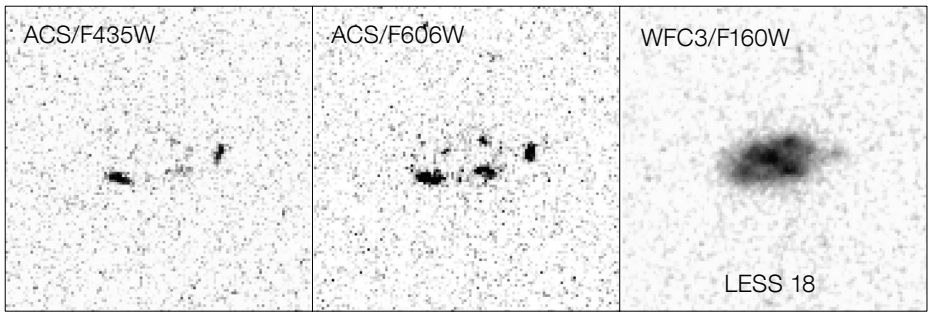


Figure 4. Detail of one of the sources, LESS 18, showing how it breaks up into several clumps at short wavelengths. The UV clumps do not appear to suffer from large extinction, while the central part of the galaxy only shows up at longer wavelengths, perhaps resulting from patchy dust obscuration.

## Conclusions

The sensitivity and high angular resolution provided by ALMA are clearly illustrated by the first SMG observations in Cycle 0, and it promises a bright future for this type of study. The optical/NIR counterparts of the ten SMGs within the CANDELS GOODS-S field show that, in contrast to local ULIRGs, there are only a few cases of ongoing mergers and most appear to be isolated systems. Furthermore, the SMGS clearly have a "history" as portrayed by their evolved stellar populations. While the redshift range of the SMGs discussed here ranges from $z = 1.65$ to $z = 4.76$, the overall stellar masses and dust masses are remarkably homogeneous, with the exception of two sources LESS 10 and LESS 34.

If the discrepant properties of LESS 10 and LESS 34 can be explained by the submm emission from a background source, while the designated counterpart is in the foreground, then it shows that even with the improved capability provided by ALMA, there are still cases where the identification of the optical/NIR counterpart of an SMG remains elusive. This situation is similar to the very first SMG detected in the Hubble Deep Field, HDF850.1, for which no optical/NIR counterpart has yet been identified despite a tremendous observational effort; the redshift is now known from molecular emission lines (Walter et al., 2012). A similar technique can be used on the SMGs observed with ALMA and will be the ultimate arbiter of whether the submm emission is associated with the designated optical/NIR counterparts or not.

## References


Ashby, M. L. N. et al. 2013, ApJ, 769, 80
Aretxaga, I. et al. 2007, MNRAS, 379, 1571
Blain, A. W. & Longair, M. S. 1993, MNRAS, 264, 509
Bruzual, G. & Charlot, S. 2003, MNRAS, 344, 1000
Chapman, S. C. et al. 2003, Nature, 422, 695
Conselice, C. J. et al. 2003, ApJS, 147, 1
Donley, J. L. et al. 2010, ApJ, 719, 1393
Fontana, A. et al. 2014, The Messenger, 155, 42
Grogin, N. A. et al. 2011, ApJS, 197, 35
Guo, Y. G. et al. 2013, ApJS, 207, 24
Hodge, J. A. et al. 2013, ApJ, 768, 91
Hughes, D. H. et al. 1998, Nature, 394, 241
Koekemoer, A. M. et al. 2011, ApJS, 197, 36
Lee, S.-K. et al. 2010, ApJ, 725, 1644
Lotz, J. M. et al. 2008, ApJ, 672, 177
Magnelli, B. et al. 2011, A&A, 528, 35
Scoville, N. Z. et al. 2014, ApJ, 783, 84
Smail, I. et al. 1997, ApJ, 490, L5
Swinbank, M. et al. 2012, The Messenger, 149, 40
Targett, T. A. et al. 2013, MNRAS, 432, 2012
Walter, F. et al. 2012, Nature, 486, 233
Weiss, A. et al. 2009, ApJ, 707, 1201
Wiklind, T. et al. 2014, ApJ, 785, 111